Pulse Splitting for Harmonic Beamforming in Time-Modulated Linear Arrays

L. Poli, T. Moriyama, P. Rocca

Abstract

In this paper, a novel strategy for harmonic beamforming in time-modulated linear arrays is proposed. The pulse splitting technique is exploited to simultaneously generate two harmonic patterns, one at the central frequency and another at a preselected harmonic of arbitrary order, while controlling the maximum level of the remaining sideband radiations. An optimization strategy based on the Particle Swarm Optimizer is developed in order to determine the optimal parameters describing the pulse sequence used to modulate the excitation weights of the array elements. Representative numerical results are reported and discussed pointing out potentialities and limitations of the proposed approach.

1 Mathematical Formulation

Let us consider a linear array of N elements aligned along the z-axis whose uniform excitation amplitudes vary in time according to a periodic modulation function $C(t)$ with period T_p, composed by Q rectangular pulses defining in which portions of the modulation period the elements are in active (*on*) or inactive (*off*) state, as shown in Fig. 1. The time-varying array factor can be calculated as

$$F(\theta,t) = e^{j\omega_0 t} \sum_{n=1}^{N} C(t) e^{j\beta(n-1)d\cos(\theta)} \tag{1}$$

where ω_0 is the angular working frequency of the antenna, $\beta = 2\pi/\lambda$ is the wavenumber, d is the interelement spacing and $\theta \in [0 : 180]$ degrees. By expanding $C(t)$ in a Fourier series, eq. (1) becomes

$$F(\theta,t) = e^{j\omega_0 t} \sum_{n=1}^{N} \left\{ \sum_{h=-\infty}^{+\infty} c_{hn} e^{j\omega_p t} \right\} e^{jk(n-1)d\cos(\theta)} \tag{2}$$

where $\omega_p = 2\pi/T_p$ and the complex Fourier coefficients c_{hn} ($h \in \mathbb{Z}$) can be computed as follows

$$c_{hn} = \frac{1}{T_p} \int_0^{T_p} C(t) e^{-jh\omega_p t} dt = \frac{j}{2\pi h} \sum_{q=1}^{Q} \left[e^{jh\omega_p \tau_{nq}^F} - e^{jh\omega_p \tau_{nq}^R} \right] \tag{3}$$

being τ_{nq}^R and τ_{nq}^F the rise instant and the fall instant normalized with respect to the modulation period T_p of the q-th sub-pulse related to n-th waveform, respectively ($q = 1,...,Q$ and $n = 1,...,N$). The pattern generated in far-field at the angular frequency $\omega_h = (\omega_0 + h\omega_p)$ is expressed as

$$F(\theta)|_{\omega_h} = \sum_{n=1}^{N} c_{hn} e^{jk(n-1)d\cos(\theta)}. \tag{4}$$

Dealing with the central angular frequency ω_0, it can be easily proved that the array factor

$F(\theta)|_{\omega_0}$ turns out to be

$$F(\theta)|_{\omega_0} = \sum_{n=1}^{N} \left[\sum_{q=1}^{Q} \left(\tau_{nq}^{F} - \tau_{nq}^{R} \right) \right] e^{jk(n-1)d\cos(\theta)} \tag{5}$$

2 PSO-based Synthesis Strategy

The optimization strategy is aimed to simultaneously synthesize a beam pattern at the working angular frequency ω_0 oriented along the broadside direction $\theta^{\omega_0} = 90^o$ and a beam pattern at a selected frequency $\omega_{\hat{h}} = (\omega_0 + \hat{h}\omega_p)$, $\hat{h} \in \mathbb{Z}_0$, steered toward an arbitrary direction $\theta^{\omega_{\hat{h}}} \in [0^o : 180^o]$. The PSO algorithm which has already provided effective results in the synthesis of time-modulated arrays has been applied to determine the optimized split pulse sequences exciting the uniform weigths of the array elements. The parameters describing such pulse sequences pictorially described in Fig. 1 are the rise and the fall instants of the rectangular sub-pulses normalized to T_p, $\underline{\tau}^R = \left\{ \tau_{nq}^R; n = 1,...,N; q = 1,...,Q \right\}$ and $\underline{\tau}^F = \left\{ \tau_{nq}^F; n = 1,...,N; q = 1,...,Q \right\}$, respectively. However, since the optimization must provide results subject to physical rules about the sequence of the sub-pulses [i.e., $\left(\tau_{nq}^F \geq \tau_{nq}^R \right); q = 1,...,Q, n = 1,...,N$ and $\left(\tau_{nq}^R \geq \tau_{n(q-1)}^F \right); q = 2,...,Q, n = 1,...,N$], in order to simplify the implementation of the constraints to be considered during the optimization process, the following variables will be optimized: $\underline{\tau}^D = \left\{ \tau_{nq}^D; n = 1,...,N; q = 1,...,Q \right.$ and $\underline{\tau}^S = \left\{ \tau_{nq}^S; n = 1,...,N; q = 1,...,Q \right\}$, which represent the sub-pulse durations and the temporal shift among two adjacent sub-pulses (i.e., τ_{nq}^S represents the time delay between the sub-pulses q and $(q-1)$ or the delay between the sub-pulse q and the origin if $q = 1$) normalized to T_p, respectively. Accordingly, the constraints can be simply recast to [$\left(\tau_{nq}^D \geq 0 \right)$ and $\left(\tau_{nq}^S \tau_{nq}^R \geq 0 \right); q = 1,...,Q, n = 1,...,N$]. The total number of variables to be optimized turns out to be $X = 2NQ$.

- **Step 1 - Parameters Setup:**

  (a) Definition of the desired pattern features described in terms of sidelobe level ($SLL_{trg}^{\omega_h}$, $h = 0, \hat{h}$) first null beam width ($\Theta_{trg}^{\omega_h}$, $h = 0, \hat{h}$), desired peak level evaluated along θ^{ω_h} ($Peak_{trg}^{\omega_h}$ $h = 0, \hat{h}$) and undesired sideband level ($SBL_{trg}^{\omega_{\overline{h}}}$ $\overline{h} = 1,...,H, \overline{h} \neq \hat{h}$);

(b) Setting of the PSO parameters: number of agents (M), maximum number of iterations (K), inertial weight (I), cognitive and social acceleration coefficients (C_1 and C_2, respectively), and convergence threshold (χ);

(c) Definition of the research ranges for the unknown variables: $\tau_{nq}^{D} \in \left[\tau_{nq}^{D,min} : \tau_{nq}^{D,max}; \; n = 1,...,N; q = 1,...,Q\right]$ and $\tau_{nq}^{S} \in \left[\tau_{nq}^{S,min} : \tau_{nq}^{S,max}; \; n = 1,...,N; q = 1,...,Q\right]$.

- **Step 2 - Swarm Initialization:** The particles of the swarm are randomly generated except of a single particle whose entries are analytically determined, in order to speed up the convergence of the optimization process, as follows:

(a) the parameters $\underline{\tau}^{D}$ and $\underline{\tau}^{S}$ have been initially set to $\tau_{nq}^{D} = \hat{\tau}^{D}$ and $\tau_{nq}^{S} = \hat{\tau}^{S}$ ($n = 1,...,N; q = 1,...,Q$) where $\left(\hat{\tau}^{D}; \hat{\tau}^{S}\right)$ represents the couple of parameters which allows to obtain the maximum value of the ratio Γ [eq. (7)], evaluated for a limited set of combinations of the trial parameters $\tau^{D} \in \left\{\left(\tau^{D,max} - \tau^{D,min}\right) m/D_{trial}; m = 1,...,D_{trial}\right\}$ and $\tau^{S} \in \left\{\left(\tau^{S,max} - \tau^{S,min}\right) m/S_{trial}; m = 1,...,S_{trial}\right\}$:

$$\left(\hat{\tau}^{D}; \hat{\tau}^{S}\right) = \left(\tau^{D}, \tau^{S}\right) \Leftrightarrow \max_{\left(\tau^{D}, \tau^{S}\right)} \{\Gamma\} \tag{6}$$

being

$$\Gamma = \frac{SBL^{\omega_{\hat{h}}}}{\sum_{h=1, h\neq\hat{h}}^{H} SBL^{\omega_h}} \tag{7}$$

being SBL^{ω_h} the maximum level of the pattern associated to ω_h;

(b) the split pulse sequence is then shifted in order to steer the beam pattern generated at the angular frequency $\omega_{\hat{h}}$ along the desired direction $\theta^{\omega_{\hat{h}}}$:

$$\begin{cases} \tau_{nq}^{D} = \hat{\tau}^{D} & n = 1,...,N; q = 1,...,Q \\ \tau_{nq}^{S} = \hat{\tau}^{S} + \frac{(n-1) d_{\lambda} \cos(\theta^{\omega_h})}{\hat{h}} & n = 1,...,N; q = 1,...,Q \end{cases} \tag{8}$$

where d_λ is the interelement distance expressed in wavelength.

- **Step 3 - Optimization Process**: The cost function defined in the following will be iteratively computed in order to evaluate if the shape of the multi-beam pattern of the optimized configuration meets the requirements defined through the target pattern parameters initialized in the Step 1(a). It can be expressed as the summation of three main terms:

$$\Psi^{(k)}\left(\underline{\tau}^D,\underline{\tau}^S\right)=\Psi_D^{(k)}\left(\underline{\tau}^D,\underline{\tau}^S\right)+\Psi_U^{(k)}\left(\underline{\tau}^D,\underline{\tau}^S\right)+\Psi_P^{(k)} \tag{9}$$

where $\Psi_D^{(k)}$ is the term aimed at shaping the multi-beam pattern according to the parameters $SLL_{trg}^{\omega_h}$, $\Theta_{trg}^{\omega_h}$ and $Peak_{trg}^{\omega_h}$ ($h=0,\hat{h}$) that is defined as follows

$$\Psi_D^{(k)}\left(\underline{\tau}^D,\underline{\tau}^S\right)=\sum_{\gamma\in\Upsilon}\alpha_\gamma\left\{\sum_{h=0,\widehat{h}}\left[\left(\frac{\left|\gamma^{\omega_h}-\gamma_{trg}^{\omega_h}\right|^2}{\left|\gamma_{trg}^{\omega_h}\right|^2}\right)\mathscr{H}\left(\gamma^{\omega_h}-\gamma_{trg}^{\omega_h}\right)\right]\right\} \tag{10}$$

where $\Upsilon=\{SLL,\Theta,Peak\}$ and $\mathscr{H}$ is the Heaviside function, whose argument has inverted sign when $\gamma\leftarrow Peak$; the term $\Psi_U^{(k)}$ is devoted to handle the undesired sideband radiation limiting the maximum sideband level,

$$\Psi_U^{(k)}\left(\underline{\tau}^D,\underline{\tau}^S\right)=\alpha_U\max_{\theta,\overline{h}}\left\{\frac{\left|F(\theta)|_{\omega_{\overline{h}}}\right|^2}{\left|F(\theta)|_{\omega_0}\right|^2}\right\},\ \theta\in[0^\circ:180^\circ];\overline{h}=1,...,H,\overline{h}\neq\hat{h} \tag{11}$$

finally, the term $\Psi_P^{(k)}=\alpha_P\mathscr{H}\left(\left[\Sigma_{q=1}^{Q}\left(\tau_{nq}^S+\tau_{nq}^S\right)\right]-1\right)$ is a penalty factor introduced to discard the solutions which provide meaningless configurations (i.e., when $\left[\Sigma_{q=1}^{Q}\left(\tau_{nq}^S+\tau_{nq}^S\right)>1\right]$). Moreover, α_γ ($\gamma\in\Upsilon$), α_U and α_P are real weighting coefficients and k is the *PSO* iteration index.

3 Numerical Results

Some representative experiments are presented in this Section in order to show potentialities and limitations of the proposed technique, by addressing the synthesis of multi-beam pattern at the central angular frequency (ω_0) and at a selected harmonic frequency ($\omega_{\hat{h}}$).

Let us consider an arrangement of $N = 16$ elements displaced along the z-axis and equally-spaced of $d = \lambda/2$. In a preliminary example, the synthesis of a sum beam pattern at the central angular frequency ω_0 in the broadside direction ($\theta^{\omega_0} = 90^o$) and a sum beam pattern at the fundamental frequency $\omega_1 = (\omega_0 + \omega_p)$ along $\theta^{\omega_1} = 120^o$ is proposed. The specific multi-beam configuration has been already investigated in [8], but in this case and unlike [8], in order to limit the loss of power, the reduction of the sideband level associated to the undesired harmonics ($\left|\bar{h}\right| = 21, ..., H, \bar{h} \neq -1, 0, 1$, being in the specific case $H = 10$) has been also taken into account during the optimization process. The target pattern features have been selected as [8] $SLL_{trg}^{\omega_0} = SLL_{trg}^{\omega_1} = -20\,dB$; $SBL_{trg}^{\omega_1} = -2\,dB$; $Peak_{trg}^{\omega_1} = -2.0\,dB$; $\Theta_{trg}^{\omega_0} = 19.6^o$, $\Theta_{trg}^{\omega_1} = 20.6^o$ (these two latter have been chosen according to the optimized result achieved in [8], in order to take into account the unavoidable slight widening of the beam width due to the steering operation). Moreover, the undesired sideband level has been fixed to $SBL_{trg}^{\omega_{\bar{h}}} = -10\,dB$. The parameters related to the optimization strategy has been selected according to [8], as well: $I = 0.4$, $C_1 = C_2 = 2.0$, $M = N$, $K = 2000$, $\chi = 10^{-5}$, $\left[\tau_{nq}^{D,min} : \tau_{nq}^{D,max}\right] = \left[\tau_{nq}^{S,min} : \tau_{nq}^{S,max}\right] = [0 : 1]$; dealing with the cost function the weighting coefficients have been set to $\alpha_\gamma = \alpha_U = 1$ ($\gamma \in \Upsilon$) and $\alpha_P = 10^3$. Finally, in order to initialize the swarm for the PSO-algorithm almost in real-time, the number of the trial solutions evaluated to analytically define one particle of the swarm has been fixed to $S_{trial} \times D_{trial} = 20 \times 20 = 400$.

The power patterns generated at ω_0 and ω_1 afforded by the optimized pulse sequence of Fig. 2(a) achieved assuming $Q = 1$ is shown in Fig. 2(b). As expected, the optimization of durations and time-shifts of simple rectangular pulsed waveforms allows to obtain a desired multi-beam radiation pattern that fulfills the given requirements, as can be seen from the data reported in Tab. I (i.e., $SLL_{PSO,Q=1}^{\omega_o} = -21.06\,dB$ vs. $SLL_{trg}^{\omega_o} = -20.00\,dB$ and $SLL_{PSO,Q=1}^{\omega_1} = -20.00\,dB$ vs. $SLL_{trg}^{\omega_1} = -20.00\,dB$; $Peak_{PSO,Q=1}^{\omega_1} = -2.0\,dB$ vs. $Peak_{trg}^{\omega_1} = -2.0\,dB$; $\Theta_{PSO,Q=1}^{\omega_0} = 18.8^o$ vs. $\Theta_{trg}^{\omega_0} = 19.6^o$ and $\Theta_{PSO,Q=1}^{\omega_1} = 20.6$ vs. $\Theta_{trg}^{\omega_1} = 20.6^o$). Moreover, the additional term in the

cost function defined in (11) and aimed to control the undesired harmonic radiations allowed to obtain an improvement in terms of sideband level ($SBL^{\omega_{\bar{h}}}_{PSO,Q=1} = -9.5\,dB$ vs. $SBL^{\omega_{\bar{h}}}_{\overline{PSO}} = -6.44\,dB$, where the subscript $\overline{PSO}$ is related to the technique presented in [8]) and also in terms of useful power (expressed in percentage on the total radiated power) associated to the pattern synthesized at ω_0 and ω_1 as can be seen in Fig. 3, (i.e., $P^{\omega_0}_{PSO,Q=1} = 33.88\%$ vs. $P^{\omega_0}_{\overline{PSO}} = 30.50\%$ and $P^{\omega_1}_{PSO,Q=1} = 21.41\%$ vs. $P^{\omega_1}_{\overline{PSO}} = 20.70\%$), in spite of a lower level of the pattern generated at the fundamental frequency ω_1 ($SBL^{\omega_1}_{PSO,Q=1} = -2\,dB$ vs. $SBL^{\omega_1}_{\overline{PSO}} = -1.5\,dB$).

The synthesis problem has been addressed also considering split pulsed waveforms, setting $Q = 2$ or $Q = 3$, but in the specific case no significant improvements have been obtained with respect to the result reached with the single-pulse rectangular waveforms. In fact, Tab. I shows that the configurations achieved for $Q = 2$ and $Q = 3$ provide a pattern at ω_0 with lower sidelobe level and narrower beam width (i.e., $SLL^{\omega_o}_{PSO,Q=2} = -21.70\,dB$ and $SLL^{\omega_0}_{PSO,Q=3} = -21.21\,dB$ vs. $SLL^{\omega_0}_{PSO,Q=1} = -21.06\,dB$; $\Theta^{\omega_0}_{PSO,Q=2} = \Theta^{\omega_0}_{PSO,Q=3} = 18.2^o$ vs. $\Theta^{\omega_0}_{PSO,Q=1} = 18.8^o$), but such solutions bring to an higher waste of power in the SRs (i.e., $SR_{PSO,Q=2} = 50.3\%$ and $SR_{PSO,Q=3} = 48.6\%$ vs. $SR_{PSO,Q=3} = 44.7\%$).

Unlike the previous case, the single-pulse rectangular waveforms do not provide satisfactory results when synthesizing the second beam pattern at a harmonic angular frequency of higher order ($|h| > 1$). Let us consider in the second example the synthesis of two sum beam patterns at the angular frequencies ω_0 and $\omega_3 = (\omega_0 + 3 \cdot \omega_p)$, ($\hat{h} = 3$). The target pattern features have been selected as in the previous case ($SLL^{\omega_0}_{trg} = SLL^{\omega_3}_{trg} = -20\,dB$; $SBL^{\omega_3}_{trg} = -2\,dB$; $\Theta^{\omega_0}_{trg} = 19.6^o$, $\Theta^{\omega_3}_{trg} = 20.6^o$ and $SBL^{\omega_{\bar{h}}}_{trg} = -10\,dB$). The optimized solution and the associated radiation power patterns are reported in Fig. 4(a) and Fig. 4(b), respectively. Although the beam patterns have been almost perfectly shaped according to the input requirements as shown in Fig. 4(b), the undesired sideband level turns out to be very high, $SBL^{\omega_{\bar{h}}}_{PSO,Q=1} = -2.77\,dB$. Indeed, as shown in Fig. 5, most of the power is lost in the unusable radiation, and the useful power associated to the patterns synthesized at ω_0 and ω_3 is limited to a small percentage of the total amount $(P^{\omega_0}_{PSO,Q=1} + P^{\omega_3}_{PSO,Q=1}) = 9.9\% + 7.1\% = 17\%$.

Dealing with the same synthesis problem, more effective results can be obtained by setting the number of sub-pulses to $Q = 3$, considering split rectangular waveforms. The op-

timized pulse sequence turns out to be as in Fig. 6(a) affording a multi-beam radiation reported in Fig. 6(b), that widely satisfy the initial requirements (Tab. II). Fig. 7(a) shows as the optimization of the split pulses allows to selectively distribute the power among the harmonic frequencies, comparing the power associated to each harmonic when $Q = 1$ (i.e., without splitting) and $Q = 3$. Similar considerations arise from the observation of the comparison in terms of sideband level in Fig. 7(b). As a matter of fact, by analyzing the undesired radiation at ω_1 and ω_2, it is possible to observe that the sideband level decreases from $SBL^{\omega_1}_{PSO,Q=1} = -2.77\,[dB]$ to $SBL^{\omega_1}_{PSO,Q=3} = -14.92\,[dB]$ and from $SBL^{\omega_2}_{PSO,Q=1} = -3.25\,[dB]$ to $SBL^{\omega_2}_{PSO,Q=3} = -15.92\,[dB]$, respectively. Moreover, the maximum sideband level is also reduced of $\Delta SBL = \left|SBL_{PSO,Q=1} - SBL_{PSO,Q=3}\right| = |-10.00 + 2.77| = -7.23\,[dB]$.

However, it is worth of noting that similar performance can be obtained avoiding the optimization of complex split rectangular waveforms. Indeed, starting from the optimized pulse sequence achieved in the preliminary example, described by the parameters $\widetilde{\tau}^R_{nq}$ and $\widetilde{\tau}^F_{nq}$ ($n = 1,...,N$; $q = 1$) which allows to synthesize the multi-beam pattern at ω_0 and $\omega_1 = (\omega_0 + \omega_p)$ of Fig. 2(b), it is possible to easily derive the parameters of the split waveforms with $Q = \hat{h}$ affording the generation of the second beam pattern at an arbitrary angular harmonic frequency $\omega_{\hat{h}} = (\omega_0 + \hat{h} \cdot \omega_p)$, through

$$\begin{cases} \tau^R_{nq} = \frac{\widetilde{\tau}^R_{nq} + (q-1)}{\hat{h}} \\ \tau^F_{nq} = \frac{\widetilde{\tau}^F_{nq} + (q-1)}{\hat{h}} \end{cases} \quad n = 1,...,N; q = 1,...,\hat{h} \tag{12}$$

Therefore, the pattern previously generated at ω_1 will be reproduced at $\omega_{\hat{h}}$, nullifying the radiation at the frequencies $\omega_h \in \left\{(\omega_0 + h \cdot \omega_p);\, h \neq q \cdot \hat{h};\, |h| = 1,...,\infty;\, |q| = 0,...,\infty\right\}$, but giving rise to a spreading of the harmonic spectrum (i.e., the pattern previously generated at ω_h, $|h| = 1,...,\infty$, will be shifted to $\omega_{h \cdot \hat{h}}$). Dealing with the case for $\hat{h} = 3$, the analytically calculated parameters of the adapted split waveforms are reported in Fig. 8(a), whereas the radiation patterns are shown in Fig. 8(b).

However, eq. (12) shows that the durations of the sub-pulses of the split waveforms depend on $\hat{h}$, and more specifically the higher the harmonic index $\hat{h}$, the shorter the durations of the sub-pulses. Accordingly, pulses with very short durations (i.e., very small fractions of the

modulation period T_p) could arise from the necessity to shift the pattern to an harmonic frequency of high order (e.g., $\hat{h} > 3$) and could be hard to realize in practice. However, since the proposed optimization strategy does not require to fix the number of sub-pulses according to the harmonic index $\hat{h}$ of the selected frequency, it can be profitably employed to synthesize the multi-beam radiation previously investigated through simpler waveforms (i.e., with $Q = 2 < \hat{h}$). In fact, the beam patterns shown in Fig. 9(b) are generated by the split pulse sequence having a number of sub-pulses limited to $Q = 2$ graphically described in Fig. 9(a). At the expense of a higher amount of power lost in the SRs ($SR_{PSO,Q=2} = 66.0\%$ vs. $SR_{\widetilde{PSO},Q=3} = 44.7\%$, being the subscript $\widetilde{PSO}$ related to the analytically derived solution of Fig. 8(a)-(b)), the optimization approach provides a solution characterized by a pulse sequence less complicated to implement, concerning the number of sub-pulses ($Q_{PSO} = 2$ vs. $Q_{\widetilde{PSO}} = 3$) and the minimum duration of the pulses of the waveforms exciting the elements of the array (directly related to the maximum speed of the RF switches used to implement the modulating function $C(t)$), as well ($\min_{n,q}\left\{\tau_{nq}^{PSO,Q=2}\right\} = 9.5 \times 10^{-2}$ vs. $\min_{n,q}\left\{\tau_{nq}^{\widetilde{PSO},Q=3}\right\} = 4.3 \times 10^{-2}$).

4 Conclusions

A multi-beam pattern synthesis technique has been proposed in this paper. A PSO-based strategy has been effectively employed to determine the optimal split pulse sequence aimed at syntesizing multiple patterns at different frequencies. The following considerations can be remarked from the analysis of the numerical results presented in the previous Section:

- Multiple patterns can be simultaneously synthesized at the central frequency and at an arbitrarily selected harmonic frequency, through the PSO-based strategy by applying the pulse splitting technique;
- An higher index $\hat{h}$ related to the synthesis of the second harmonic beam pattern requires more complicated waveforms to implement. The complexity of the split waveforms can be relaxed at expense of an higher amount of losses in the unused radiation.

Future efforts will be devoted to the extension of the proposed approach to the planar case, and to study the possibility do define alternative waveforms more suitable for the specific purpose.

References

[1] L. Poli, P. Rocca, L. Manica, A. Massa, “Handling sideband radiations in time-modulated arrays through particle swarm optimization,” *IEEE Trans. Antennas Propag.*, vol. 58, no. 4, pp. 1408-1411, Apr. 2010.

[2] L. Poli, P. Rocca, L. Manica, A. Massa, “Time modulated planar arrays - Analysis and optimisation of the sideband radiations,” *IET Microw. Antennas Propag.*, vol. 4, no. 9, pp. 1165-1171, 2010.

[3] P. Rocca, L. Poli, G. Oliveri, A. Massa, “Synthesis of time-modulated planar array with controlled harmonic radiations,” *J. Electromagn. Waves Appl.,* vol. 24, no. 4, pp. 827-838, 2010.

[4] P. Rocca, L. Poli, G. Oliveri, and A. Massa, “Synthesis of sub-arrayed time modulated linear arrays through a multi-stage approach,” *IEEE Trans. Antennas Propag.*, vol. 59, no. 9, pp. 3246-3254, Sep. 2011.

[5] L. Poli, P. Rocca, and A. Massa, “Sideband radiation reduction exploiting pattern multiplication in directive time-modulated linear arrays,” *IET Microw. Antennas Propag.*, vol. 6, no. 2, pp. 214-222, 2012.

[6] E. T. Bekele, L. Poli, M. D’Urso, P. Rocca, and A. Massa, “Pulse-shaping strategy for time modulated arrays - Analysis and design,” *IEEE Trans. Antennas Propag.*, vol. 61, no. 7, pp. 3525-3537, Jul. 2013.

[7] L. Poli, P. Rocca, L. Manica, A. Massa, “Pattern synthesis in time-modulated linear arrays through pulse shifting,” *IET Microw. Antennas Propag.*, vol. 4, no. 9, pp. 1157-1164, 2010.

[8] L. Poli, P. Rocca, G. Oliveri, and A. Massa, “Harmonic beamforming in time-modulated linear arrays,” *IEEE Trans. Antennas Propag.*, vol. 59, no. 7, pp. 2538-2545, Jul. 2011.

[9] P. Rocca, L. Poli, G. Oliveri, and A. Massa, "A multi-stage approach for the synthesis of sub-arrayed time modulated linear arrays," IEEE Trans. Antennas Propag., vol. 59, no. 9, pp. 3246-3254, Sep. 2011.

[10] P. Rocca, L. Poli, G. Oliveri, and A. Massa, "Adaptive nulling in time-varying scenarios through time-modulated linear arrays," IEEE Antennas Wireless Propag. Lett., vol. 11, pp. 101-104, 2012.

[11] P. Rocca, L. Poli, and A. Massa, "Instantaneous directivity optimization in time-modulated array receivers," IET Microwaves, Antennas & Propagation, vol. 6, no. 14, pp. 1590-1597, Nov. 2012.

[12] P. Rocca, L. Poli, L. Manica, and A. Massa, "Synthesis of monopulse time-modulated planar arrays with controlled sideband radiation," IET Radar, Sonar & Navigation, vol. 6, no. 6, pp. 432-442, 2012.

[13] L. Poli, P. Rocca, G. Oliveri, and A. Massa, "Adaptive nulling in time-modulated linear arrays with minimum power losses," IET Microwaves, Antennas & Propagation, vol. 5, no. 2, pp. 157-166, 2011.

[14] P. Rocca, L. Poli, G. Oliveri, and A. Massa, "Synthesis of time-modulated planar arrays with controlled harmonic radiations," Journal of Electromagnetic Waves and Applications, vol. 24, no. 5/6, pp. 827-838, 2010.

[15] L. Manica, P. Rocca, L. Poli, and A. Massa, "Almost time-independent performance in time-modulated linear arrays," IEEE Antennas Wireless Propag. Lett., vol. 8, pp. 843-846, 2009.

[16] P. Rocca, L. Manica, L. Poli, and A. Massa, "Synthesis of compromise sum-difference arrays through time-modulation," IET Radar, Sonar & Navigation, vol. 3, no. 6, pp. 630-637, 2009.

[17] P. Rocca, M. D'Urso, and L. Poli, "An iterative approach for the synthesis of optimized sparse time-modulated linear arrays," Progress In Electromagnetics Research B, vol. 55, pp. 365-382, 2013.

[18] L. Poli, P. Rocca, G. Oliveri, and A. Massa, "Failure correction in time-modulated linear arrays," IET Radar, Sonar & Navigation, vol. 8, no. 3, pp. 195-201, 2014. doi:10.1049/iet-rsn.2013.0027.

[19] L. Poli, T. Moriyama, and P. Rocca, "Pulse splitting for harmonic beamforming in time-modulated linear arrays," International Journal of Antennas and Propagation, vol. 2014, pp. 1-9, 2014.

FIGURE CAPTIONS

- **Figure 1.** Example of split pulse controlling a *RF* switch.

- **Figure 2.** *Single-Pulse Waveform,* $Q = 1$ - *Multi-Beam Sum Pattern Synthesis at* ω_0 *and* ω_1 ($N = 16$; $d = \lambda/2$; $\theta^{\omega_0} = 90^o$; $\theta^{\omega_1} = 120^o$) - Plot of (*a*) the optimized pulse sequence and (*b*) corresponding power patterns generated at ω_0, ω_1, ω_2 *and* ω_3.

- **Figure 3.** *Single-Pulse Waveform,* $Q = 1$ - *Multi-Beam Sum Pattern Synthesis at* ω_0 *and* ω_1 ($N = 16$; $d = \lambda/2$; $\theta^{\omega_0} = 90^o$; $\theta^{\omega_1} = 120^o$) - Plot of the power associated to the harmonic radiations in percentage on the total power.

- **Figure 4.** *Single-Pulse Waveform,* $Q = 1$ - *Multi-Beam Sum Pattern Synthesis at* ω_0 *and* ω_3 ($N = 16$; $d = \lambda/2$; $\theta^{\omega_0} = 90^o$; $\theta^{\omega_3} = 120^o$) - Plot of (*a*) the optimized pulse sequence and (*b*) corresponding power patterns generated at ω_0, ω_1, ω_2 *and* ω_3.

- **Figure 5.** *Single-Pulse Waveform,* $Q = 1$ - *Multi-Beam Sum Pattern Synthesis at* ω_0 *and* ω_3 ($N = 16$; $d = \lambda/2$; $\theta^{\omega_0} = 90^o$; $\theta^{\omega_3} = 120^o$) - Plot of the power associated to the harmonic radiations in percentage on the total power.

- **Figure 6.** *Multi-Pulse Waveform,* $Q = 3$ - *Multi-Beam Sum Pattern Synthesis at* ω_0 *and* ω_3 ($N = 16$; $d = \lambda/2$; $\theta^{\omega_0} = 90^o$; $\theta^{\omega_3} = 120^o$) - Plot of (*a*) the optimized pulse sequence and (*b*) corresponding power patterns generated at ω_0, ω_1, ω_2 *and* ω_3.

- **Figure 7.** *Comparative Assessment - Single-Pulse Waveform,* $Q = 1$ vs. *Multi-Pulse Waveform,* $Q = 3$ ($N = 16$; $d = \lambda/2$; $\theta^{\omega_0} = 90^o$; $\theta^{\omega_3} = 120^o$) - Plot of (*a*) the power associated to the harmonic radiations in percentage on the total power and (*b*) the sideband level associated to the harmonic patterns.

- **Figure 8.** *Multi-Pulse Waveform,* $Q = 3$ - *Multi-Beam Sum Pattern Synthesis at* ω_0 *and* ω_3 ($N = 16$; $d = \lambda/2$; $\theta^{\omega_0} = 90^o$; $\theta^{\omega_3} = 120^o$) - Plot of (*a*) the analytically derived pulse sequence and (*b*) corresponding power patterns generated at ω_0, ω_1, ω_2 *and* ω_3.

- **Figure 9.** *Multi-Pulse Waveform,* $Q = 2$ - *Multi-Beam Sum Pattern Synthesis at* ω_0 *and* ω_3 ($N = 16$; $d = \lambda/2$; $\theta^{\omega_0} = 90^o$; $\theta^{\omega_3} = 120^o$) - Plot of (*a*) the optimized pulse sequence

and (b) corresponding power patterns generated at ω_0, ω_1, ω_2 *and* ω_3.

TABLE CAPTIONS

- **Table I.** *Multi-Beam Sum Pattern Synthesis at* ω_0 *and* ω_1 ($N = 16$; $d = \lambda/2$; $\theta^{\omega_0} = 90^o$; $\theta^{\omega_1} = 120^o$) - Pattern features for $Q = 1$, $Q = 2$ and $Q = 3$.

- **Table II.** *Multi-Beam Sum Pattern Synthesis at* ω_0 *and* ω_3 ($N = 16$; $d = \lambda/2$; $\theta^{\omega_0} = 90^o$; $\theta^{\omega_3} = 120^o$) - Pattern features for $Q = 1$, $Q = 2$ and $Q = 3$.

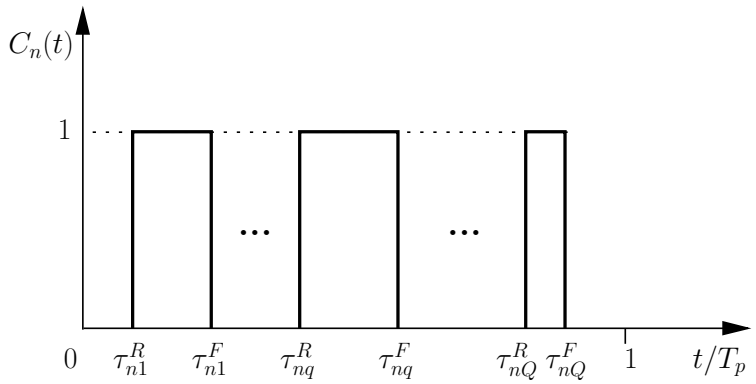

Fig. 1 - P. Rocca *et al.,* "Pulse Splitting for Harmonic Beaforming..."

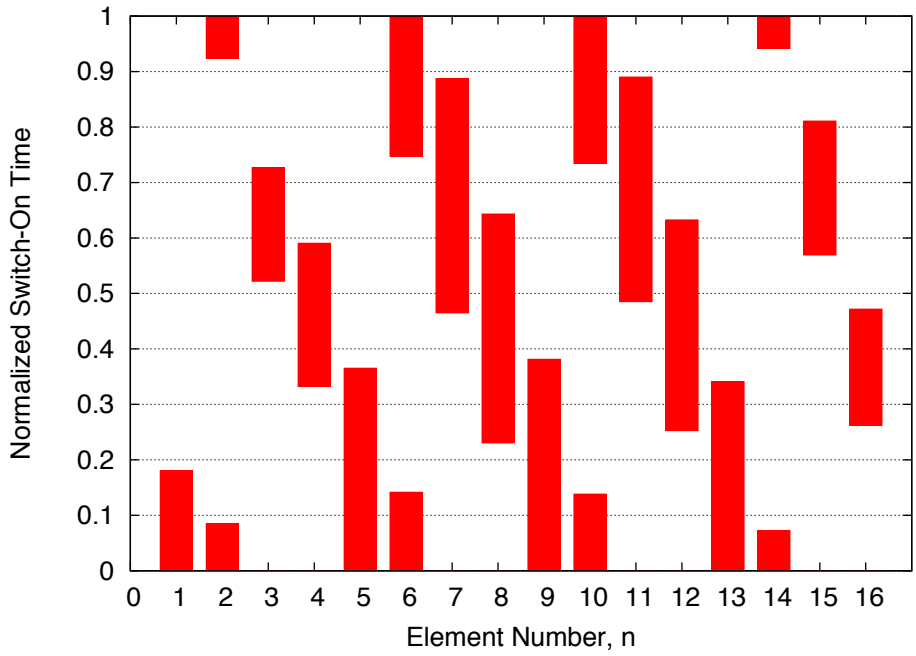

(a)

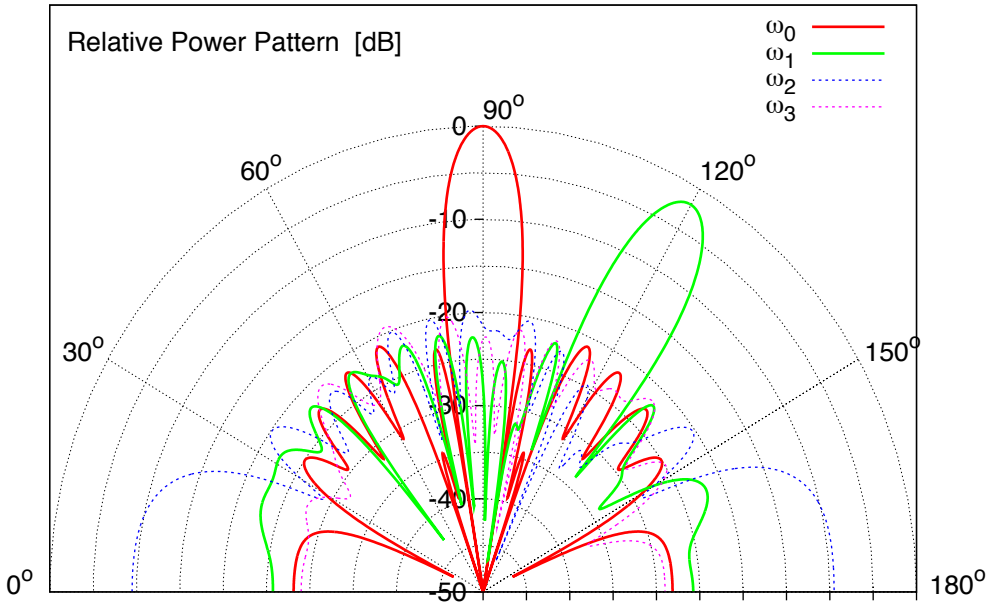

(b)

Fig. 2 - P. Rocca *et al.,* "Pulse Splitting for Harmonic Beaforming..."

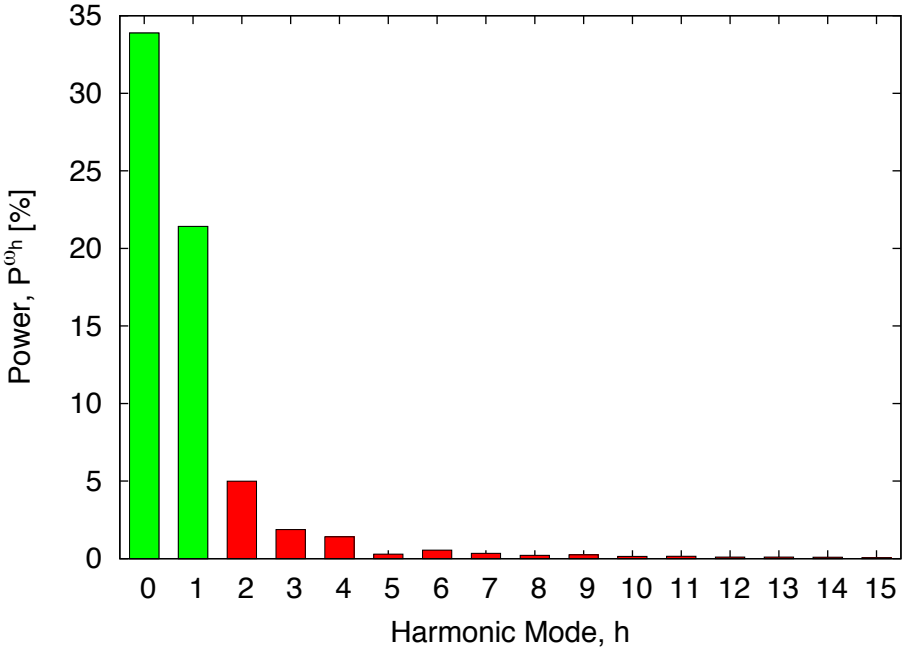

Fig. 3 - P. Rocca *et al.,* "Pulse Splitting for Harmonic Beaforming..."

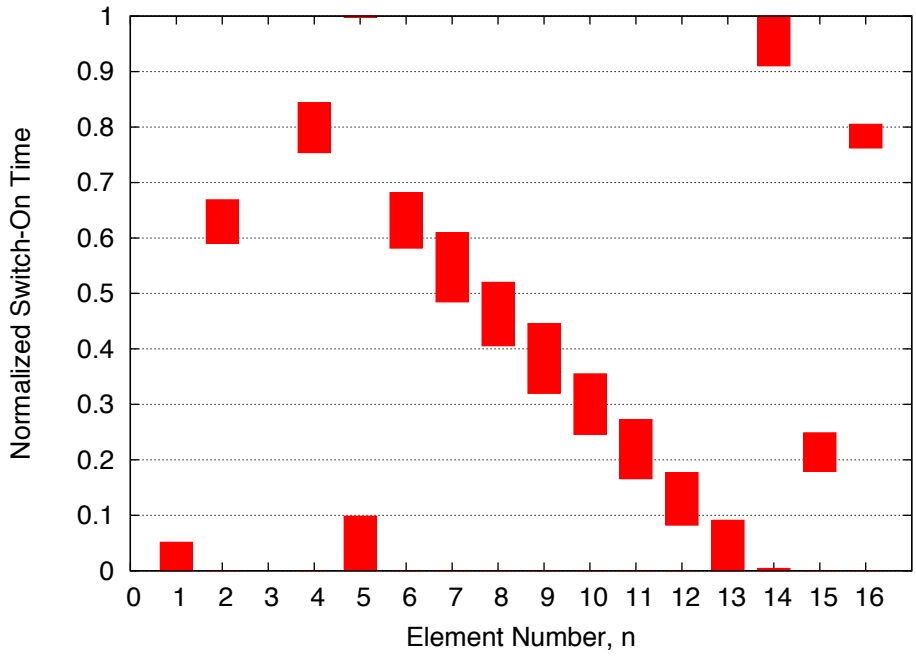

(*a*)

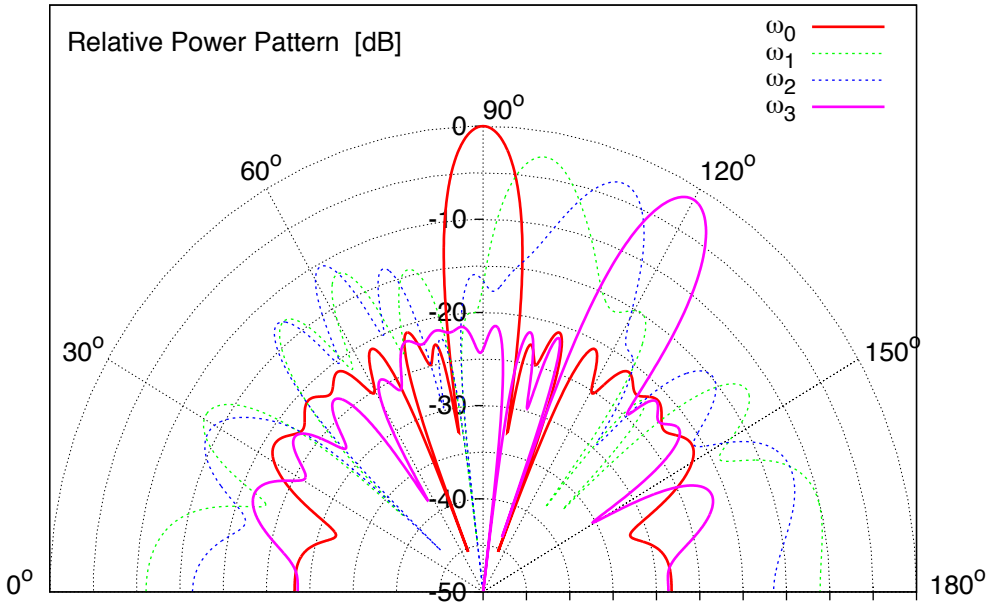

(*b*)

Fig. 4 - P. Rocca *et al.,* "Pulse Splitting for Harmonic Beaforming..."

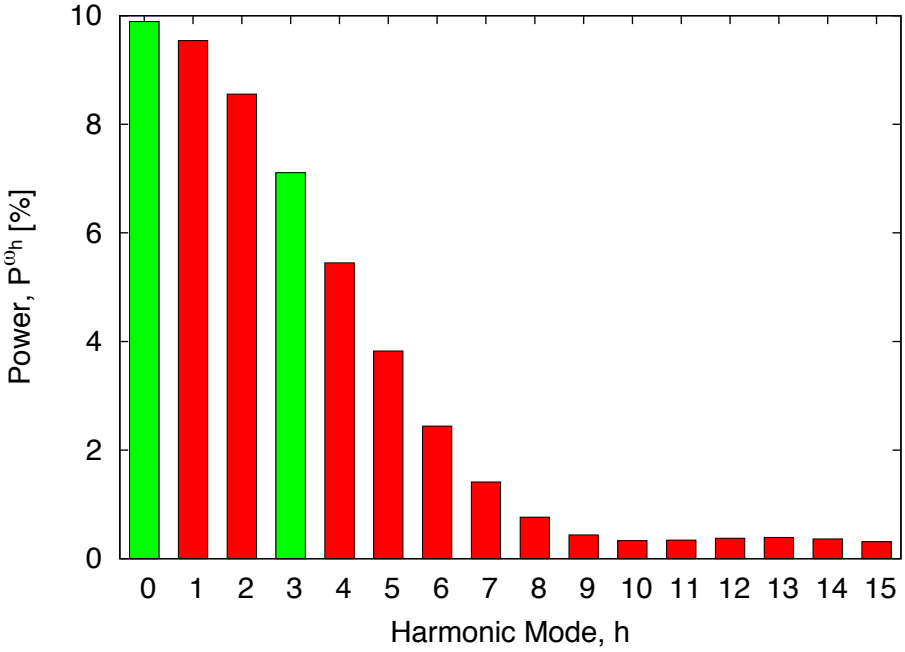

Fig. 5 - P. Rocca *et al.,* "Pulse Splitting for Harmonic Beaforming..."

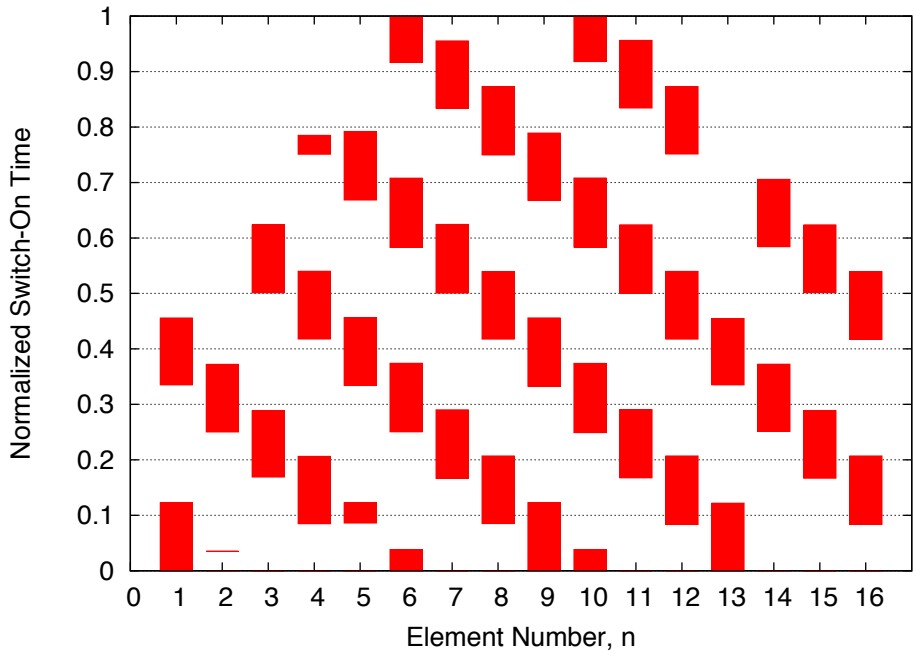

(*a*)

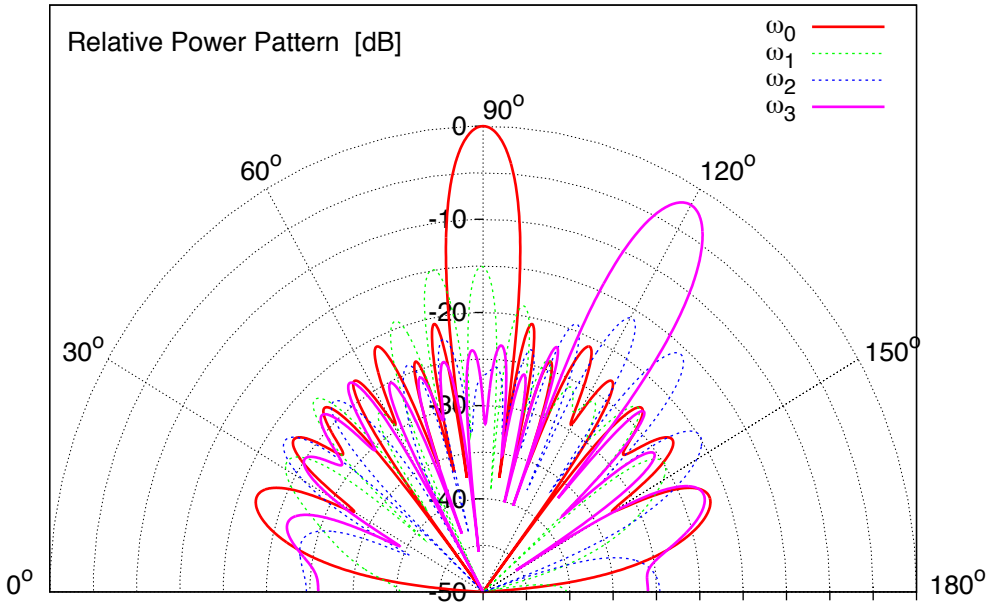

(*b*)

Fig. 6 - P. Rocca *et al.,* "Pulse Splitting for Harmonic Beaforming..."

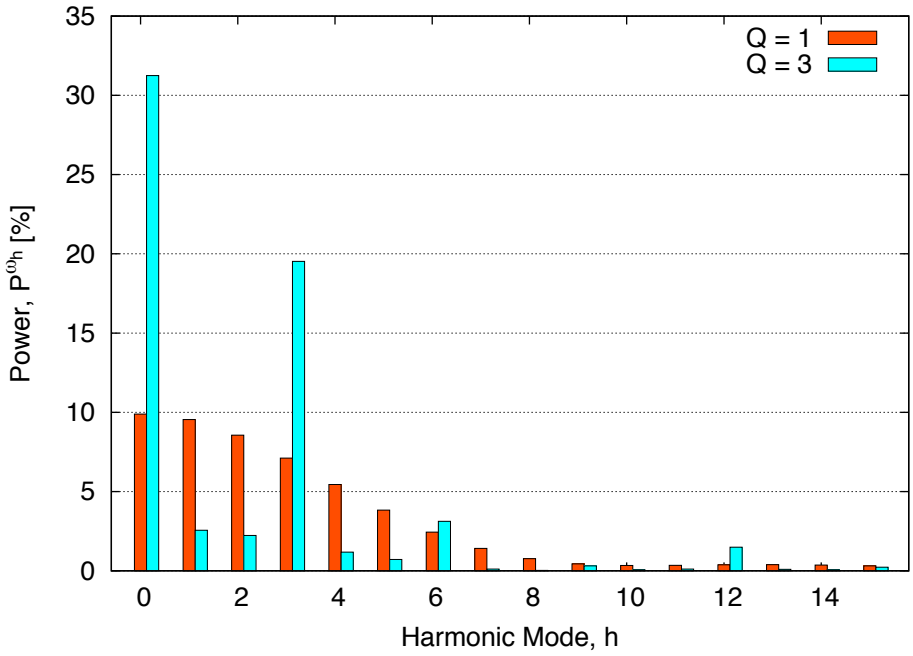

(*a*)

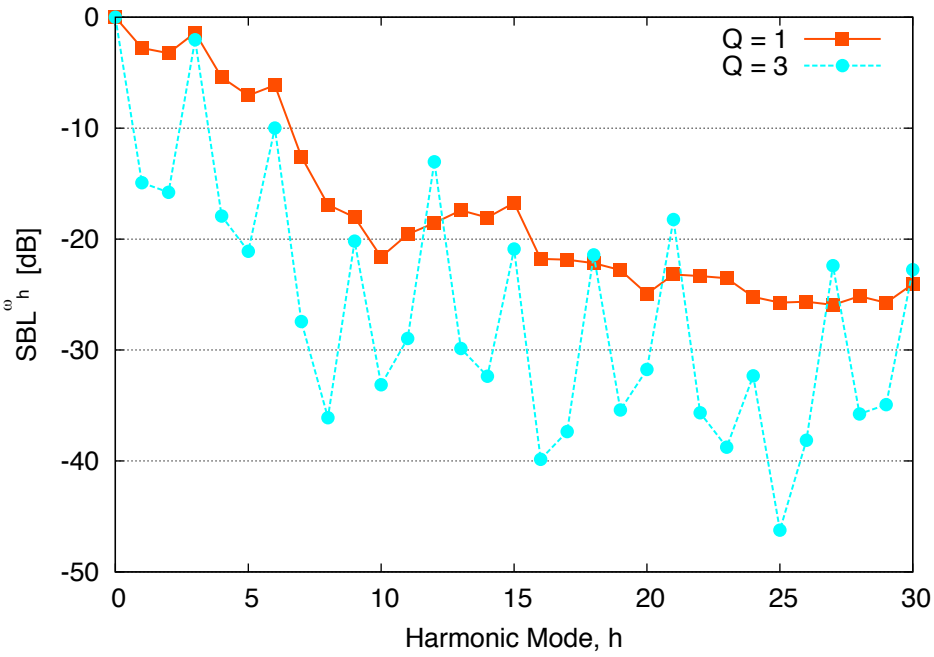

(*b*)

Fig. 7 - P. Rocca *et al.*, "Pulse Splitting for Harmonic Beaforming..."

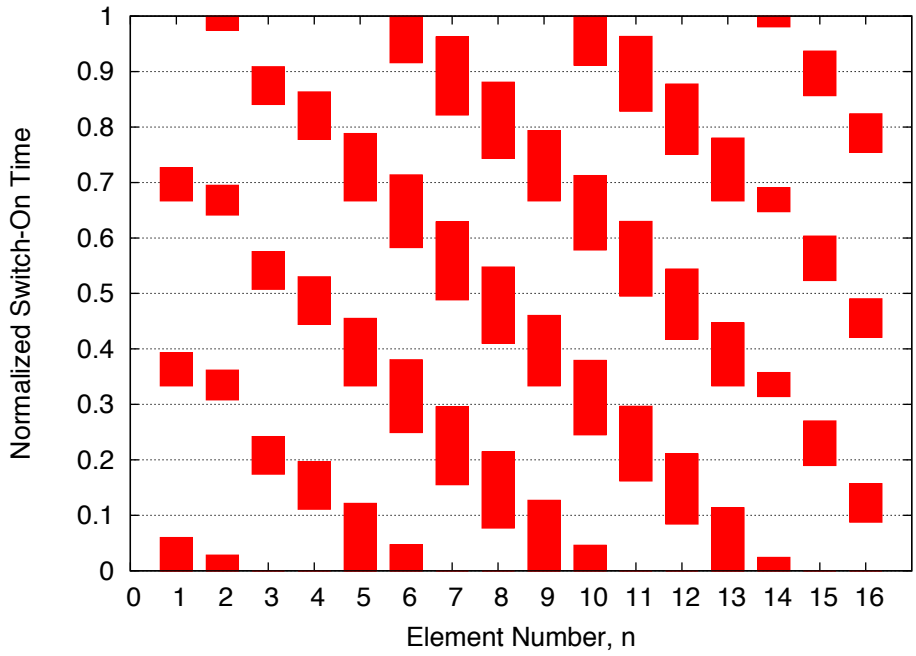

(a)

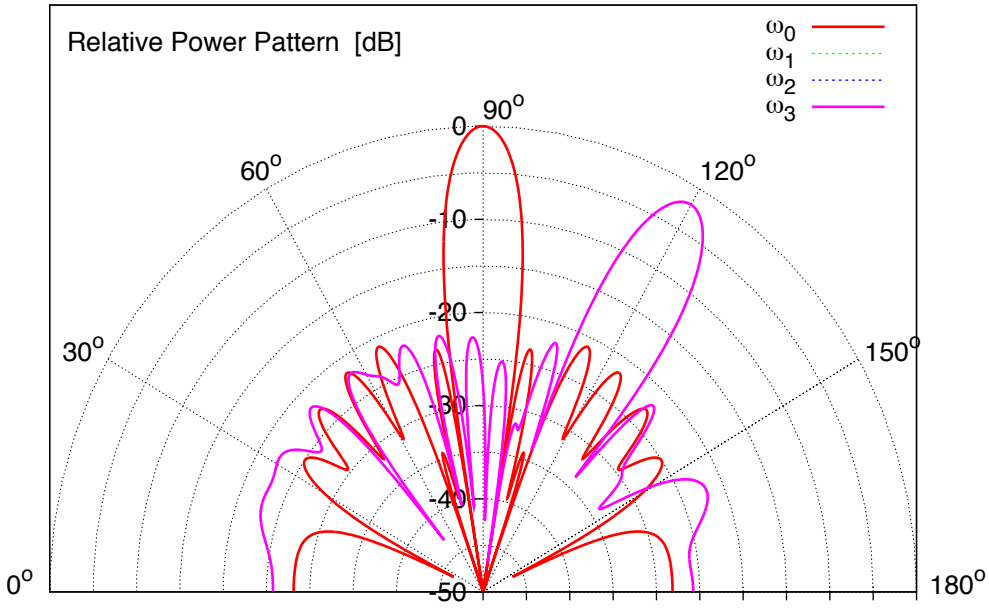

(b)

Fig. 8 - P. Rocca *et al.,* "Pulse Splitting for Harmonic Beaforming..."

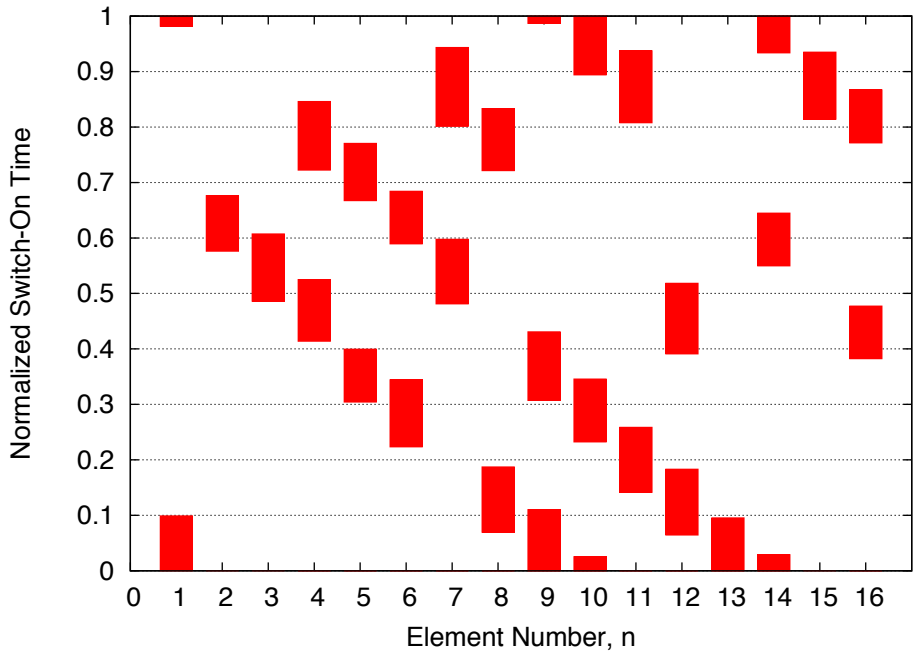

(*a*)

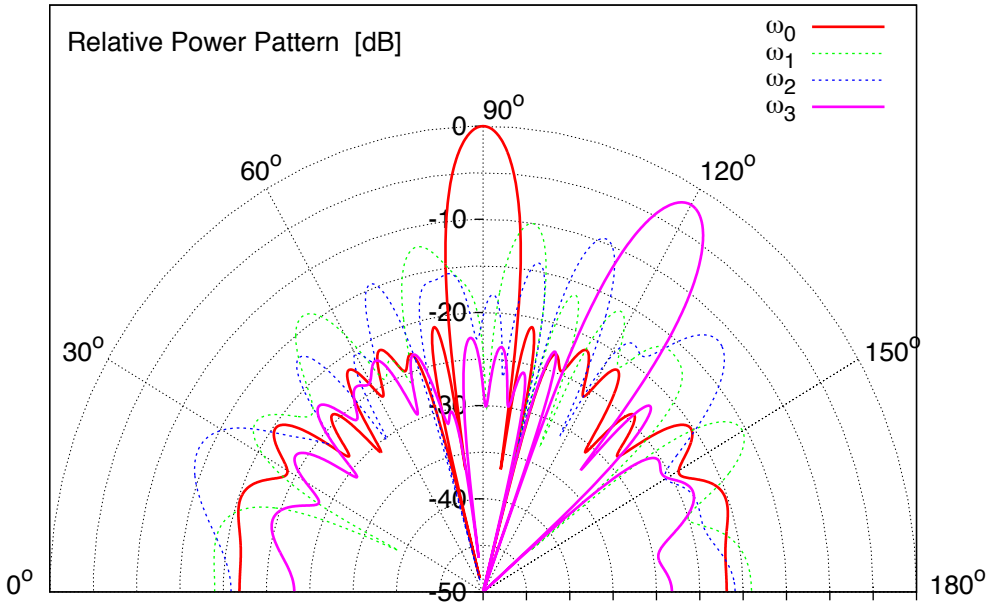

(*b*)

Fig. 9 - P. Rocca *et al.,* "Pulse Splitting for Harmonic Beaforming..."

	SLL^{ω_0} $[dB]$	SLL^{ω_1} $[dB]$	Θ^{ω_0} $[deg]$	Θ^{ω_1} $[deg]$	$Peak^{\omega_1}$ $[dB]$	$SBL^{\omega_{\bar{1}}}$ $[dB]$	P^{ω_0} $[\%]$	P^{ω_1} $[\%]$
$Q = 1$; $\omega_0 \cap \omega_1$	-21.06	-20.00	18.8	20.6	-2.0	-9.50	33.88	21.41
$Q = 2$; $\omega_0 \cap \omega_1$	-21.70	-20.00	18.2	20.6	-2.0	-10.00	30.41	19.33
$Q = 3$; $\omega_0 \cap \omega_1$	-21.21	-20.00	18.2	20.6	-2.0	-9.80	31.48	19.90

Table I - P. Rocca *et al.,* "Pulse Splitting for Harmonic Beaforming..."

	SLL^{ω_0} $[dB]$	SLL^{ω_3} $[dB]$	Θ^{ω_0} $[deg]$	Θ^{ω_3} $[deg]$	$Peak^{\omega_3}$ $[dB]$	$SBL^{\omega_{\bar{h}}}$ $[dB]$	P^{ω_0} $[\%]$	P^{ω_3} $[\%]$
$Q=1$; $\omega_0 \cap \omega_3$	-20.81	-20.00	18.6	20.6	-1.4	-2.77	9.89	7.11
$Q=2$; $\omega_0 \cap \omega_3$	-20.27	-20.26	17.6	20.3	-2.0	-9.50	20.91	13.08
$Q=3$; $\omega_0 \cap \omega_3$	-20.95	-20.37	17.4	20.1	-2.0	-10.00	31.28	19.60

Table II - P. Rocca *et al.,* "Pulse Splitting for Harmonic Beaforming..."